Verification of GCM-Generated Regional Seasonal Precipitation for Current Climate and of Statistical Downscaling Estimates under Changing Climate Conditions

ARISTITA BUSUIOC

National Institute of Meteorology and Hydrology, Bucharest, Romania

HANS VON STORCH AND REINER SCHNUR

Institute of Hydrophysics, GKSS Research Center, Geesthacht, Germany

(Manuscript received 21 October 1996, in final form 9 March 1998)

ABSTRACT

Empirical downscaling procedures relate large-scale atmospheric features with local features such as station rainfall in order to facilitate local scenarios of climate change. The purpose of the present paper is twofold: first, a downscaling technique is used as a diagnostic tool to verify the performance of climate models on the regional scale; second, a technique is proposed for verifying the validity of empirical downscaling procedures in climate change applications.

The case considered is regional seasonal precipitation in Romania. The downscaling model is a regression based on canonical correlation analysis between observed station precipitation and European-scale sea level pressure (SLP). The climate models considered here are the T21 and T42 versions of the Hamburg ECHAM3 atmospheric GCM run in ''time-slice'' mode. The climate change scenario refers to the expected time of doubled carbon dioxide concentrations around the year 2050.

The downscaling model is skillful for all seasons except spring. The general features of the large-scale SLP variability are reproduced fairly well by both GCMs in all seasons. The climate models reproduce the empirically determined precipitation–SLP link in winter, whereas the observed link is only partially captured for the other seasons. Thus, these models may be considered skillful with respect to regional precipitation during winter, and partially during the other seasons. Generally, applications of statistical downscaling to climate change scenarios have been based on the assumption that the empirical link between the large-scale and regional parameters remains valid under a changed climate. In this study, a rationale is proposed for this assumption by showing the consistency of the $2 \times CO_2$ GCM scenarios in winter, derived directly from the gridpoint data, with the regional scenarios obtained through empirical downscaling. Since the skill of the GCMs in regional terms is already established, it is concluded that the downscaling technique is adequate for describing climatically changing regional and local conditions, at least for precipitation in Romania during winter.

1. Introduction

The study of climate change due to the ongoing increase of greenhouse gas concentration in the atmosphere is a topical issue in climate research. General circulation models (GCMs) are the tools that are most widely used to generate scenarios of climate change for impact assessments. The GCMs supply useful information for global or large scales spanning several nodes of the GCM's global grid. It is not a priori clear how reliably a given GCM simulates regional climate on the scale of very few grid points. Naturally, GCM output cannot be directly used on the local scale of single grid points or below. However, users from, for example, agriculture and water resources often ask for information below the mesh size.

One of the reasons for the possible failure of the models on the regional scale is given by the spatial resolution, which provides an inadequate description of the structure of the earth's surface. Most climate models still operate on a T21 resolution, which is equivalent to a grid size of about 625 km $\times$ 625 km at the equator. The upcoming generation of models is integrated with a T42 resolution (of about 300 km $\times$ 300 km at the equator) and the models with the highest resolution so far (e.g., T106 of about 125 km $\times$ 125 km resolution), unfortunately, are not available for long-term experiments in the near future. Only short ''time-slice'' experiments are available (Bengtsson et al. 1995). Another reason for the difficulty of interpreting global climate model output on the regional scale is the spatially uniform parameterization of the subgrid-scale processes that is sometimes inadequate for different points of the world.

Corresponding author address: Hans von Storch, Institute of Hydrophysics, GKSS Research Centre, Max-Planck-Str. 1, D-21502 Geesthacht, Germany.
E-mail: storch@gkss.de

A possible solution for obtaining some information on the local scale from climate model output is ''downscaling'' procedures, which use dynamical or statistical models to relate large-scale information from GCMs (considered to be reliably modeled) to regional or local parameters. Each dynamical or statistical approach has its own disadvantages and advantages. A universal downscaling method valid for all variables and all regions is difficult to find (von Storch 1995b). An overview of currently used techniques is collected in a special issue of *Climate Research* (Kaas et al. 1996; Bürger 1996; Conway et al. 1996; Katz and Parlange 1996; Hewitson and Crane 1996; Fuentes and Heimann 1996).

In this paper a statistical downscaling procedure based on canonical correlation analysis (CCA) as proposed by von Storch et al. (1993) is used. Similar procedures have been proposed by Wigley et al. (1990), Karl et al. (1990), and Harrison et al. (1995). Some conditions have to be satisfied for this procedure to be useful. Most importantly, the GCMs should be capable of reproducing the large-scale variability realistically. Second, the relationship between the large-scale and regional-scale parameters has to be strong; that is, the local climate parameter as estimated through the statistical model should account for a significant part of the observed total variance.

The purpose of the present paper is twofold. First, we use the downscaling technique as a diagnostic tool for verifying the performance of climate models on the regional scale. We then propose a technique for verifying the skill of empirical downscaling procedures under changing climate conditions. The case considered is seasonal precipitation in Romania, the downscaling model consists of a regression technique based on CCA using European-scale air pressure fields as predictors. The climate models are the T21 and T42 versions of the ECHAM3 atmospheric GCM of the Hamburg Max Planck Institute/German Climate Computing Center (MPI/DKRZ). The climate change scenarios refer to the expected time of doubled carbon dioxide concentrations around the year 2050.

The paper is organized as follows. Section 2 presents the data used in this study. The downscaling technique is briefly described in section 3, whereas details on the method of determining the most skillful downscaling models are contained in the appendix. In sections 4 and 5, we investigate the skill as well as the limitations of the ECHAM3 GCM (T21 and T42 resolution) with respect to simulating regional precipitation in Romania and representing its link with the large-scale circulation. In section 6, we compare the estimates of climate change with respect to precipitation in Romania as derived directly from the GCM $2 \times CO_2$ simulations and indirectly using the downscaling technique. The conclusions of the study are presented in section 7.

2. Data

Observational data used in this paper are time series of monthly precipitation totals at 14 Romanian stations and mean monthly sea level pressure (SLP) between 1901 and 1990. The location and names of the Romanian stations are displayed in Fig. 1. For SLP the area between 30°–55°N and 5°–50°E has been selected. The monthly SLP data from the National Meteorological Center (now known as the National Centers for Environmental Prediction) analyses have been supplied by the National Center for Atmospheric Research with a resolution of $5° \times 5°$ (Trenberth and Paolino 1980). For both parameters, seasonal anomalies have been computed by subtracting the long-term seasonal mean from the detrended time series.

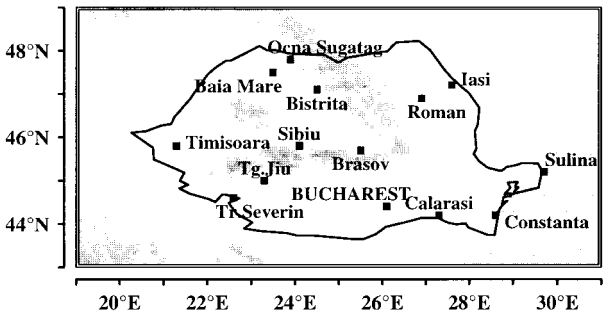

FIG. 1. Location of the 14 Romanian stations used in this study. The shading indicates the topography of the region including the Carpathian Mountains (only elevations above 500 m are marked). The gray area in the lower-right corner marks the Black Sea.

In addition, we used gridpoint SLP and precipitation from so-called time-slice simulations (T21 and T42 resolution) with the ECHAM3 atmospheric GCM run at the DKRZ (Cubasch et al. 1996). The advantage of the time-slice method is that the atmospheric model can be integrated with high resolution for several decades around a future time of interest. For this purpose, the T21, T42, and T106 ECHAM3 atmospheric models were forced with the greenhouse gas concentration corresponding to this time of interest, whereas sea surface temperature and sea ice boundary conditions were taken from a transient coarse-grid (T21) simulation of the ECHAM1/LSG coupled atmosphere–ocean model (Roeckner et al. 1992; Cubasch et al. 1992) using gradually increasing greenhouse gas concentrations according to the IPCC IS92a scenario (''business as usual''). The SST and sea-ice distributions were chosen as climatological means computed from the decade around the expected time of doubled greenhouse gas concentrations, which, in that model, occurs around model year 60 and can be linked to around 2050. Therefore, these time-slice experiments represent (high resolution) equilibrium runs for the time of doubled CO_2 and are referred to as $2 \times CO_2$ time-slice experiments. Corresponding control runs have been performed using present-day CO_2 concentrations and SST and sea ice distributions as boundary conditions and referred to as $1 \times CO_2$ time-slice experiments.

In this paper, we use a 50-yr integration of the T21 and a 30-yr integration of the T42 $2 \times CO_2$ time-slice

experiments to infer information on regional climate change under doubled CO_2 concentrations. These simulations are compared with corresponding 30-yr 1 × CO_2 time-slice control simulations. Results from the time-slice experiments at T106 resolution have not been considered here because only 5 yr of integration are available for this model, which was considered too short to confidently infer statistical information on the link between seasonal European SLP and regional precipitation. All SLP fields were interpolated from the GCM T21 and T42 Gaussian grids to the 5° × 5° grid of the SLP analyses.

3. Methods

The performance of the GCMs with respect to seasonal precipitation in Romania is assessed by comparing the gridpoint precipitation simulated by the time-slice control experiments (T21 and T42 resolution) with observed precipitation. This comparison is performed with respect to the following characteristics:

- mean state given by the long-term average of seasonal precipitation amounts
- spatial variability given by the first two empirical orthogonal function (EOF) patterns
- link between the local precipitation variability and the large-scale circulation (represented by European-scale SLP) given by the first two canonical correlation patterns (see below) of the local- and large-scale parameters.

By comparing the mean states, a potential bias in the precipitation simulation of the model can be identified. The second and third criteria involve only the anomalies from this mean state. EOF analysis is used to check if the model is able to realistically simulate the spatial variability of regional precipitation, whereas CCA is used to test for the model's representation of the main mechanisms controlling the local climate variability.

The statistical downscaling procedure proposed by von Storch et al. (1993) is used to infer local information about seasonal precipitation in Romania from the sea-level air pressure field at the European scale. This method has also been used by Werner and von Storch (1993), Gyalistras et al. (1994), Cui et al. (1995), Heyen et al. (1996), and Busuioc and von Storch (1996). It is based on CCA (Barnett and Preisendorfer 1987; von Storch 1995a), which selects pairs of spatial patterns of two space–time-dependent variables (the large-scale and the regional or local-scale climate parameter) such that their time components are optimally correlated. The first CCA pair gives the maximum correlation between the two parameters, being followed by the second CCA pair and so on. Because the coefficients are normalized to unity, the canonical correlation patterns represent the typical strength of the signal. Prior to the CCA, the original data are projected onto their EOFs thus eliminating unwanted noise and reducing the dimensions of the data space. Those EOFs that explain most of the total variance are retained for further analysis. Only EOFs explaining at least 1% from the total variance are considered.

For the purpose of downscaling, a subset of these CCA pairs is then used in a regression model to estimate the local parameter from the large-scale variable using the correlation coefficients between the respective time components. The large-scale variable can, for example, be taken as observations from a different time interval thus resulting in ''reconstructed'' local values or from GCM output. The performance of the downscaling model is sensitively dependent on the number of the EOFs retained for the CCA and the number of CCA components used in the regression model. Most commonly, the optimum number of retained EOFs is determined in such a way that using one more EOF would change the canonical correlations only a little (Werner and von Storch 1993; von Storch 1995a). In the present study, the optimum choice for the number of EOFs retained in the CCA analysis and the number of CCA time components used in the regression model has been determined simultaneously such that the skill of the model is high and does not substantially change after the addition of new components. Here, the skill of the downscaling model is expressed by the variance explained by the reconstructed local values as a fraction of the total observed variance or, alternatively, by the correlation between observed and reconstructed values. More detail on this procedure of choosing the optimal number of EOFs and CCA patterns is given in the appendix. It is only noted here that the whole observational period was divided into two subintervals and the skill of the models was considered for both the fitting period and the independent validation period. The final models that have been selected as optimal and are used in the remainder of this paper are highlighted in boldface in Table 1. Finally, it should be noted that the correlation is overestimated when obtained via CCA from a finite sample (e.g., von Storch 1995a).

4. The skill of GCMs for simulating the precipitation in Romania

In this section, we present an assessment of the performance of the ECHAM3 time-slice models with respect to regional precipitation in Romania and SLP variability on the European scale. First, the main features of the observed precipitation climate in Romania are described in section 4a in terms of long-term means and the first two EOF patterns. This climate is then compared to the precipitation as simulated by the ECHAM3 T21 and T42 time-slice control experiments. As has been mentioned in the introduction, the application of downscaling techniques to GCM results is based on the assumption that the large-scale parameter is simulated realistically by the GCM. Therefore, the first two EOFs of SLP of the observations and the two control exper-

TABLE 1. The skill of the statistical downscaling models for the two periods 1901–40 and 1941–90 and for different combinations of the number of EOFs of SLP and precipitation (PP) retained for the CCA analysis and the number of CCA pairs used in the statistical model. The model skill is expressed in terms of the (reconstructed) precipitation time series obtained from applying the downscaling model to the large-scale observed SLP fields: fraction of total variance explained by the reconstructed values, and correlation coefficient between reconstructed and observed time series (averages over all stations, respectively). The optimal combination is indicated in boldface (for spring, none of the combinations was considered skillful).

	Number of EOFs			Skill of downscaling model			
				Variant 1		Variant 2	
Season	SLP	PP	CCAs	Fitting for 1941–90	Validation for 1901–40	Fitting for 1901–40	Validation for 1941–90
Winter	2	2	2	0.57/0.77	0.24/0.60	0.35/0.59	0.41/0.72
	3	3	3	0.66/0.81	0.08/0.61	0.35/0.60	0.36/0.65
	4	4	4	0.67/0.82	0.14/0.64	0.55/0.74	0.57/0.81
	5	5	5	0.66/0.83	0.28/0.73	0.53/0.73	0.62/0.82
	6	6	5	0.72/0.85	0.28/0.67	0.54/0.74	0.62/0.83
	6	**6**	**6**	**0.79/0.89**	**0.41/0.74**	**0.57/0.75**	**0.54/0.79**
	6	7	6	0.79/0.89	0.40/0.74	0.57/0.75	0.54/0.79
Spring	2	2	2	0.29/0.54	0.07/0.29	0.38/0.62	—
	3	3	3	0.38/0.62	0.09/0.33	0.39/0.63	—
	4	4	4	0.52/0.72	0.14/0.39	0.40/0.63	−0.18/0.17
	5	5	5	0.52/0.77	0.14/0.39	0.41/0.61	−0.11/0.29
	6	6	6	0.54/0.74	0.20/0.45	0.42/0.64	−0.12/0.25
Summer	2	2	2	0.24/0.49	0.13/0.39	0.09/0.30	0.10/0.33
	3	3	3	0.24/0.49	0.10/0.35	0.09/0.30	0.10/0.33
	4	4	4	0.34/0.59	0.33/0.57	0.22/0.47	0.05/0.27
	5	5	5	0.55/0.74	0.39/0.65	0.44/0.66	0.22/0.49
	6	**6**	**5**	**0.54/0.73**	**0.41/0.66**	**0.54/0.73**	**0.35/0.61**
	6	6	6	0.56/0.75	0.35/0.63	0.54/0.73	0.32/0.59
	7	7	7	0.56/0.75	0.38/0.64	0.55/0.74	0.33/0.60
	8	8	7	0.56/0.75	0.38/0.64	0.58/0.76	0.36/0.63
Autumn	2	2	2	0.13/0.38	0.01/0.11	0.03/0.18	0.15/0.40
	3	3	3	0.13/0.30	−0.02/0.04	0.26/0.52	0.16/0.42
	4	4	4	0.17/0.64	0.15/0.54	0.44/0.69	0.31/0.60
	5	5	5	0.42/0.65	0.31/0.56	0.46/0.68	0.37/0.62
	6	**6**	**5**	**0.57/0.76**	**0.46/0.70**	**0.45/0.68**	**0.35/0.61**
	6	6	6	0.62/0.79	0.48/0.70	0.45/0.68	0.35/0.61

iments are compared in section 4b. Only the first two EOFs are discussed because these are generally describing the most important modes of variability and are considered sufficient for this purpose.

a. Regional precipitation in Romania

The interval 1941–90 has been selected as representing the current climate in Romania. The main features of the seasonal precipitation in Romania can be described as follows:

- The seasonal precipitation amount decreases from west to east with a maximum in the northwest and/or southwest (except for summer when the maximum is recorded in the northwestern and central part).
- The highest precipitation amounts are recorded in the summer and the smallest in autumn.
- The first EOF shows the same sign of variability over the entire country with a maximum in the northwest and southwest. The second EOF pattern exhibits two regions with opposite sign separated by the Carpathian chain showing the influence of the topographic structure of the Carpathians. Similar results have been presented by Draghici (1988).

As an example, the patterns of current Romanian precipitation climate are shown for the winter season. Figure 2a shows the spatial distribution of the long-term mean of the winter precipitation amount at the 14 Romanian stations. Figures 3a and 4a show the first two EOF patterns of the winter precipitation, respectively.

The precipitation fields from the T21 and T42 control run experiments were analyzed in the same manner as above. Due to the coarse GCM resolution it is difficult to do a reasonable comparison between the in situ observations and the GCM gridpoint data, especially for the T21 model. Also, GCM gridpoint values of precipitation represent areal averages rather than point values [see, e.g., Osborn and Hulme (1997) for a discussion of this issue]. Therefore, only the gross features of the spatial distributions of long-term means and EOFs are discussed.

Both models show a decrease of mean precipitation amount from west to east except for T21 in winter. The precipitation maximum in summer and minimum in au-

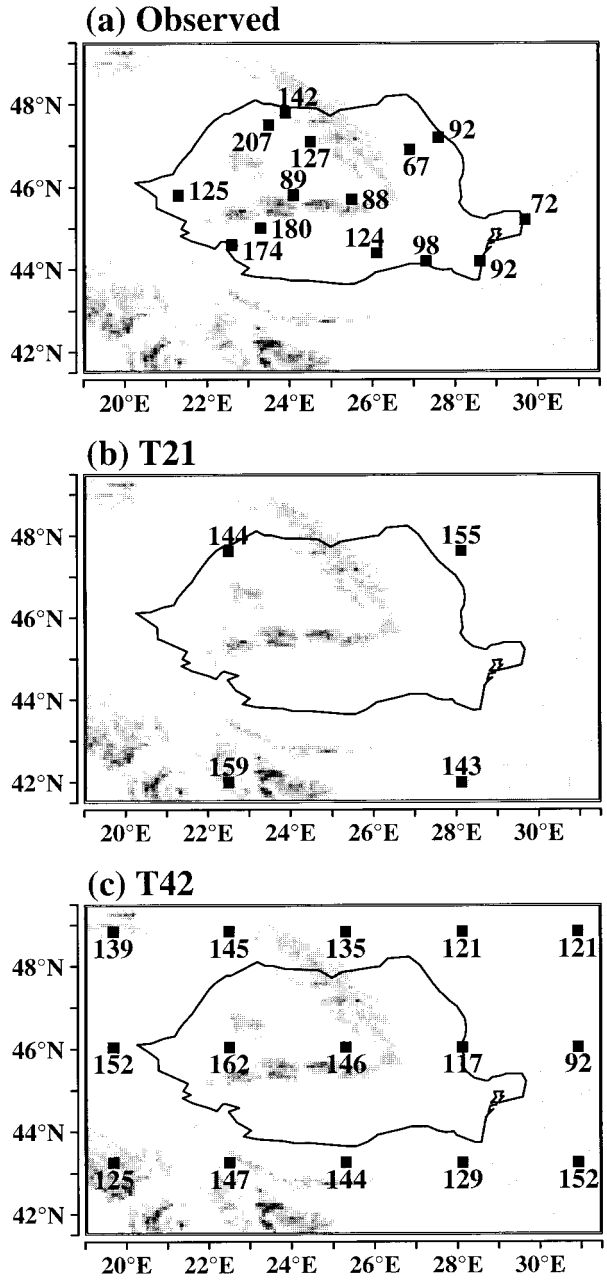

FIG. 2. Long-term mean of winter (DJF) precipitation as derived from station observations for the period 1941–90 (a) and from the gridpoint simulations of the ECHAM3 T21 (b) and T42 (c) models.

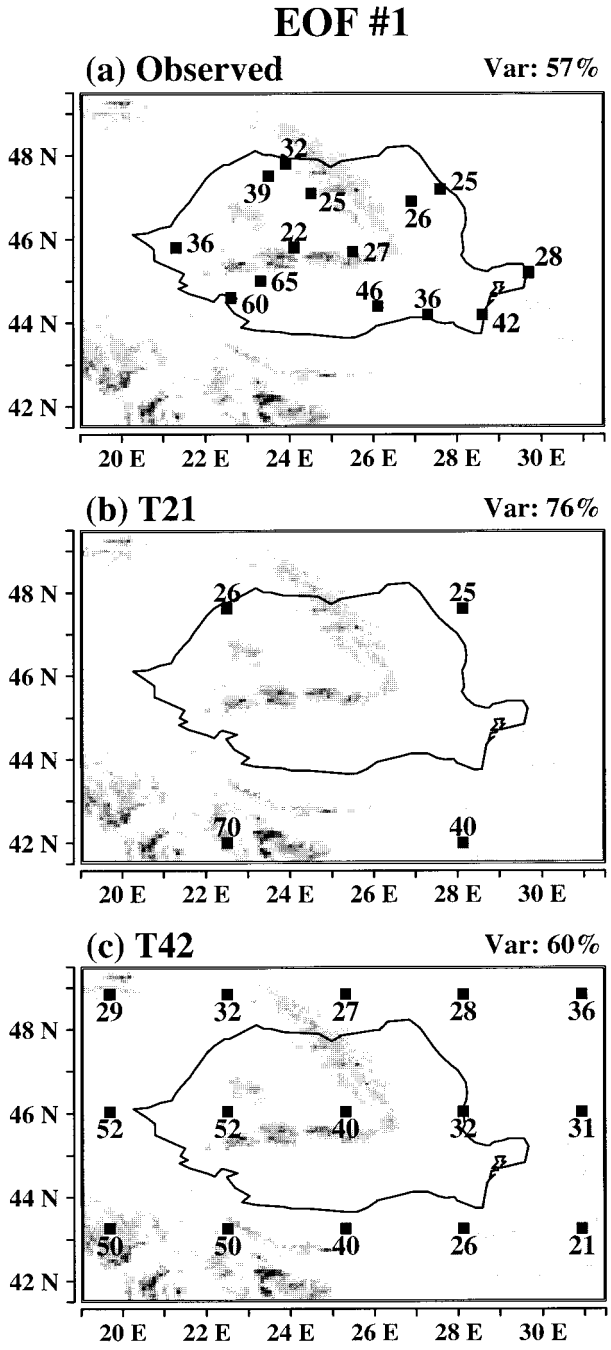

FIG. 3. The pattern of the first EOF of Romanian winter precipitation as derived from the observed seasonal amounts (a) and as derived from the seasonal amounts simulated by the ECHAM3 T21 (b) and T42 (c) models. The fraction of the respective total variance explained by each EOF is given in the upper right of each panel.

tumn are correctly reproduced only by the T21 model. Figures 2b and 2c present the spatial distributions of the long-term mean of gridpoint precipitation simulated by the T21 and T42 models, respectively, for the winter season. It can be seen that the T21 model does a poor job in simulating the west–east decrease of precipitation over Romania although the picture would get better if the information from the two southern grid points were included in computing areal averages for Romania. The T42 model captures the west–east decrease of mean precipitation although the gradient is somewhat smaller than in the observations.

The general features of the first two EOF patterns of observed seasonal precipitation in Romania are reasonably well reproduced by all models in all seasons, namely, the same sign for the first EOF and the opposite sign

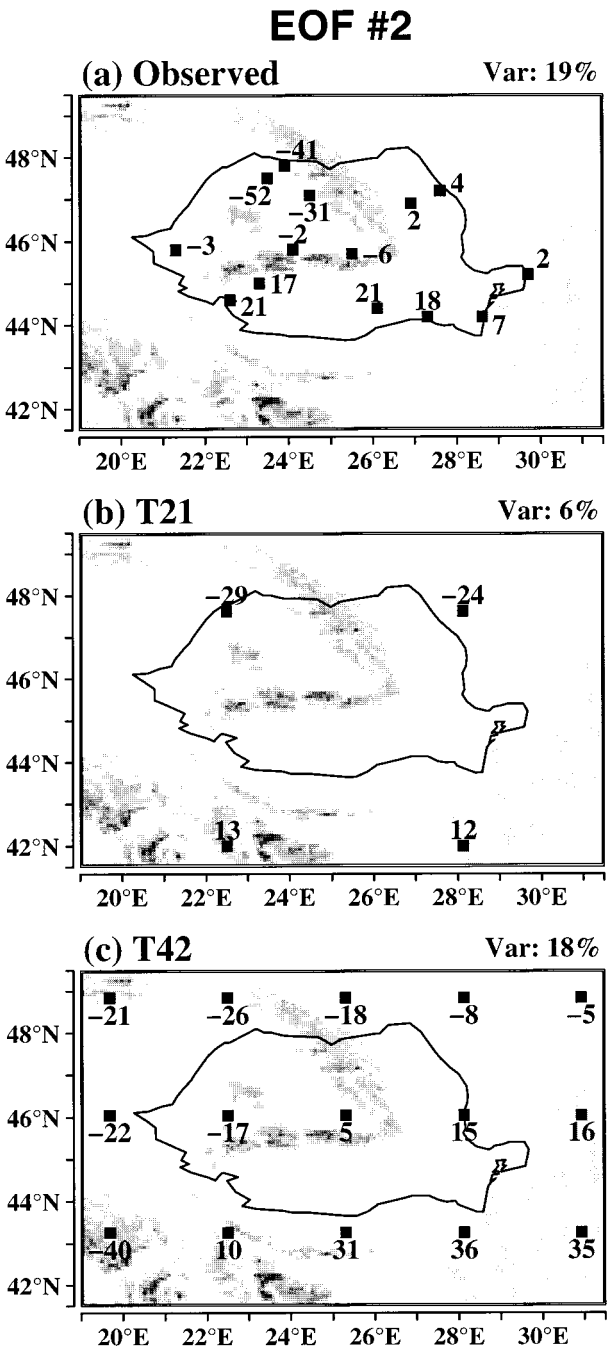

FIG. 4. As in Fig. 3 but for the second EOF of Romanian winter precipitation.

structure for the second EOF. For the winter example, the patterns of the two EOFs for the T21 and T42 control runs are shown in Figs. 3b,c and 4b,c, respectively. Similar results have been presented by Busuioc (1994) from the analysis of the Romanian gridpoint precipitation simulated by a coupled ocean–atmosphere model (T21 version of ECHAM1/LSG; Cubasch et al. 1992). In general, the good agreement between the observed and model patterns is noted. However, in the second EOF of the model outputs the Carpathians no longer mark the dividing line between negative and positive precipitation anomalies, both models simulate negative anomalies east of the Carpathians. This is most likely due to the missing or incomplete representation of this mountain range in the models, nicely illustrating the effect of the coarse resolution on regional performance.

b. Sea level pressure variability

The main features of the observed SLP fields at the European scale are presented by the first two EOF patterns. Except for the summer season, the principal mode of SLP variability (given by the first EOF pattern) is represented by a meridional circulation over Europe (see, e.g., Busuioc and von Storch 1995, 1996). During summer a zonal circulation is the principal mode of variability. The second mode is characterized by two regions of opposite sign with a northwest–southeast zero line for the winter and spring seasons, a zonal circulation for the autumn season, and a cyclonic/anticyclonic structure centered over the Black Sea for summer. Figures 5a and 6a present the first two EOF patterns for the winter season.

In comparing these observed EOF patterns with the ones obtained from the GCM simulations, one faces the fact that sometimes the patterns of the first two EOFs are similar but the order is reversed. This is only due to differences in the explained variances; that is, the models might overestimate the importance of one pattern against the other as compared to observations. Because we are interested in the main features of variability we do not discuss these discrepancies in the following but evaluate only the similarity of the patterns, regardless of order.

The T21 model reproduces the first two observed EOFs in winter and summer and only one of both in spring and autumn, respectively. For the T42 model, the first two EOFs are realistic in winter and autumn, whereas only one EOF coincides with the observed pattern in summer and spring, respectively. As an example, Figs. 5b,c and 6b,c show the first and second EOF patterns for winter derived from the T21and T42 simulations, respectively. By and large, there is good agreement between the general features of the patterns (EOF 2 of the T21 simulation has to be compared to the first observed EOF, and vice versa).

Both the precipitation (section 4a) and SLP EOFs were also computed for the 1901–40 subinterval and for the whole 1901–90 period in order to test the stability of these patterns over time. In general, the results were very similar except that, in some cases, EOF 1 and EOF 2 were switched due to slight differences in the explained variances.

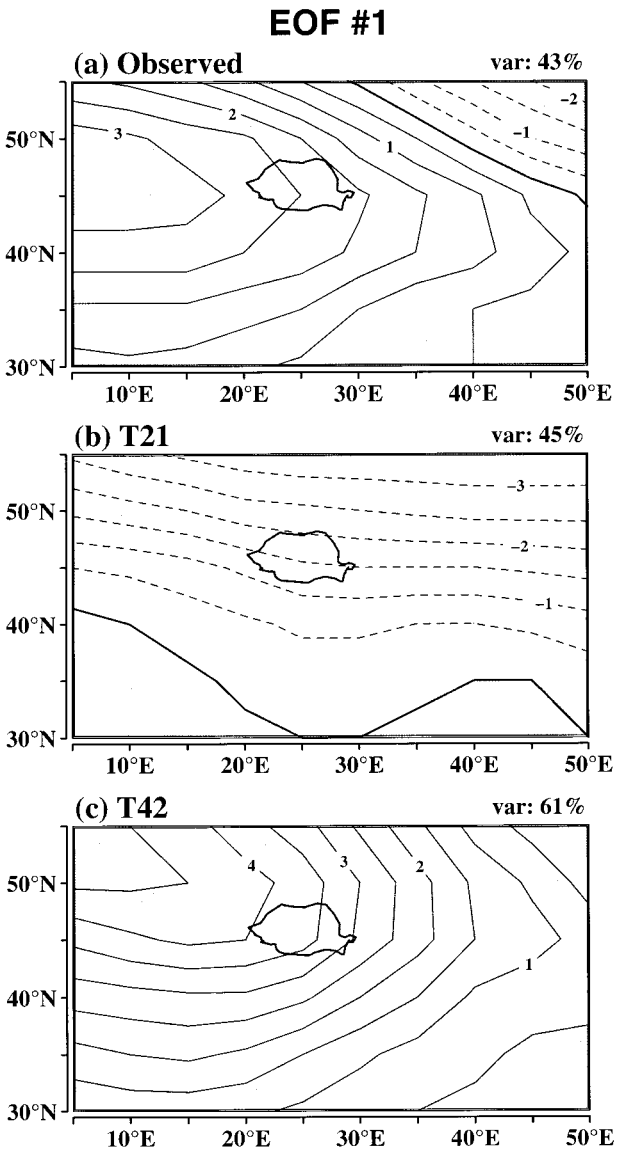

FIG. 5. The pattern of the first EOF of winter SLP as derived from the observed seasonal mean (a) and the seasonal mean simulated by the ECHAM3 T21 (b) and T42 (c) models. The fraction of the respective total variance explained by each EOF is given in the upper right of each panel. The border of Romania is outlined in solid.

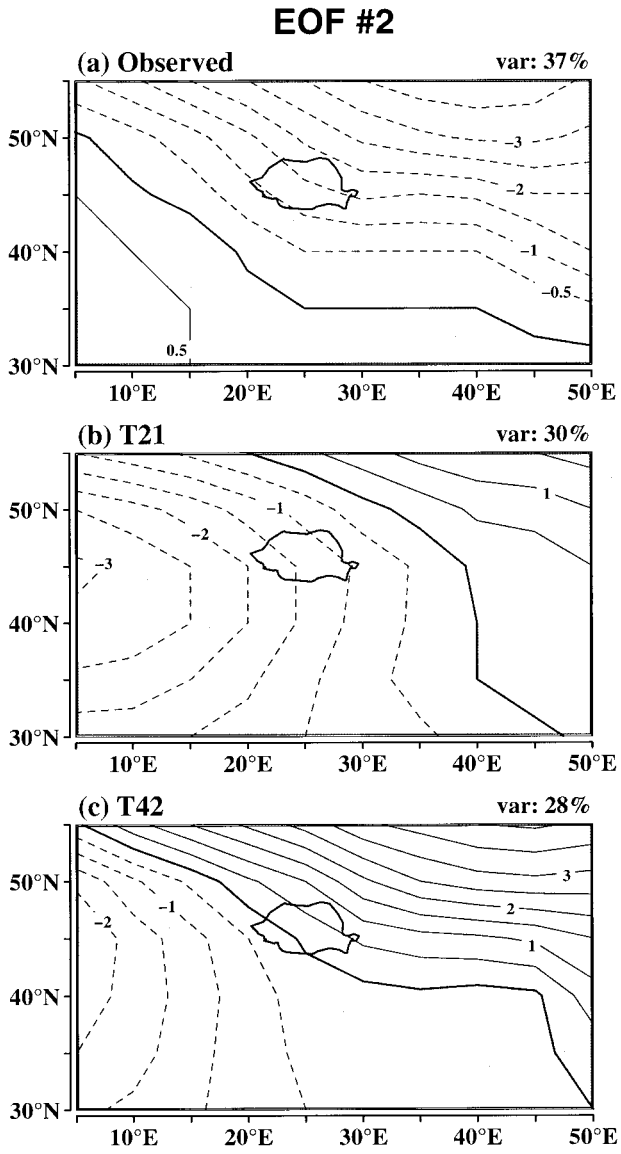

FIG. 6. As in Fig. 5 but for the second EOF of winter SLP.

5. Link between Romanian precipitation and the large-scale circulation

In section 5a, we discuss the statistical link between observed Romanian precipitation and the large-scale circulation using CCA applied to the 1941–90 interval. In section 5b, we evaluate if the T21 and T42 GCMs are able to reproduce this relationship and, thus, how well they reproduce the physical mechanisms that control regional precipitation variability. Again, similar to section 4, this link is presented in terms of only the first two canonical patterns since these are the most important (that is, those with the highest correlations between SLP and precipitation component time series). This is done for brevity but these CCA pairs are still the first two of the optimal number obtained from maximizing the skill of the downscaling model (as described in section 3 and the appendix). For both models, the number of EOFs retained for the CCA has been chosen such that addition of more EOFs did not change the CCA patterns and their correlations substantially.

a. Observed link: Construction of statistical downscaling model

The first two CCA pairs for winter for the 1941–90 period are presented in the top row of Figs. 7 and 8, respectively. They represent those patterns of SLP and precipitation with the highest and second highest cor-

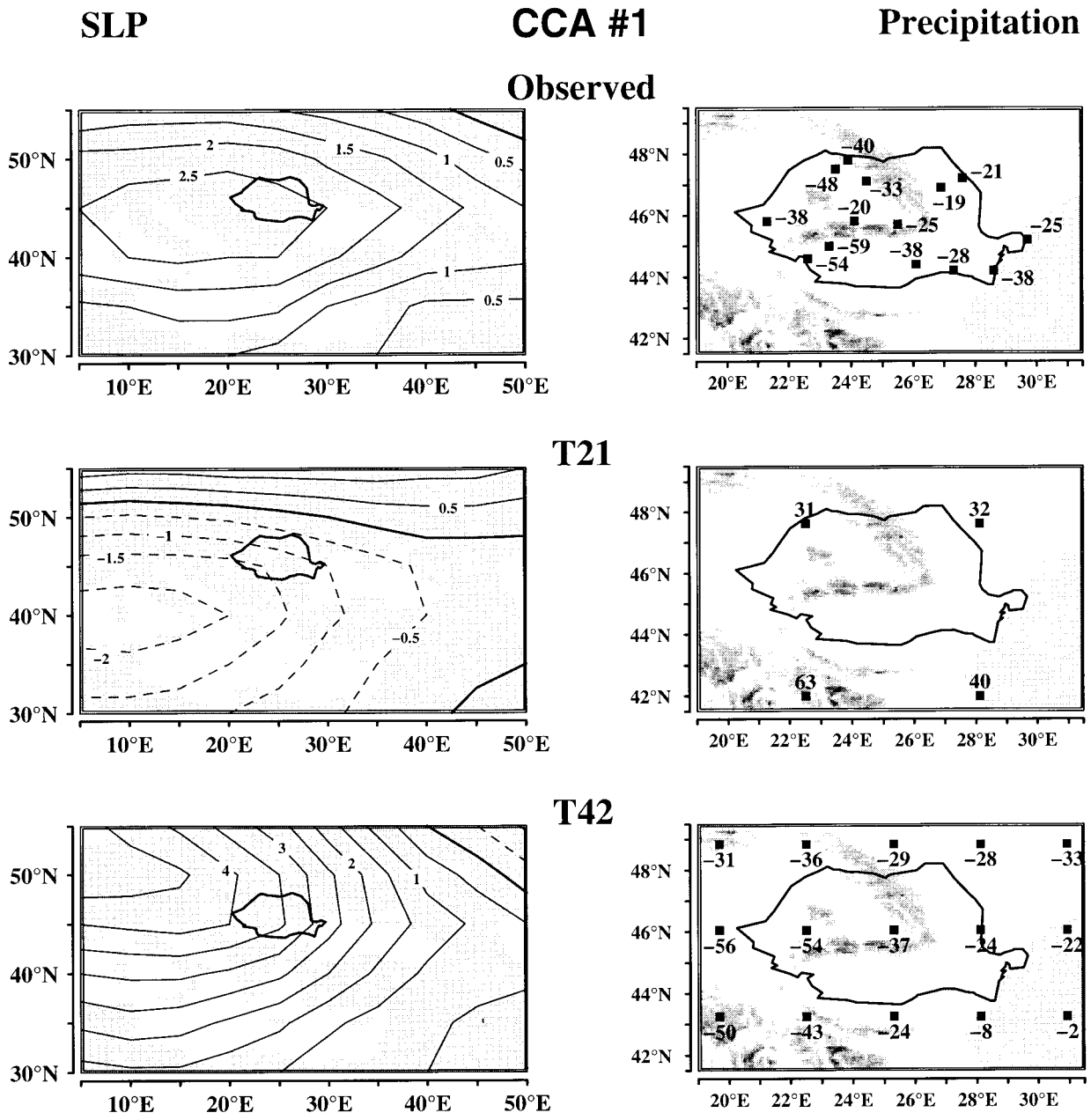

FIG. 7. The patterns of the first CCA pair of winter mean SLP (left) and winter total precipitation (right) in Romania as derived from observation (top) and simulations of the ECHAM3 T21 (middle) and T42 (bottom) models.

relation between the associated time coefficient time series satisfying the side condition that, for each variable, the first and second time coefficients are orthogonal. For the first CCA pair the correlation coefficient between the precipitation and SLP time series is 0.91. Thus, this pair associates high (low) pressure over Europe and the Mediterranean Basin (top left pattern in Fig. 7) with below- (above-) normal precipitation at the 14 stations in Romania (top right pattern in Fig. 7), which is very reasonable from a physical point of view. The SLP pattern explains 36% of the total seasonal mean SLP variance and the precipitation pattern explains 53% of the total precipitation variance. The second CCA pair (Fig. 8) (0.80 correlation coefficient between the precipitation and SLP coefficient time series) associates a southeasterly (northwesterly) flow over Romania with above (below) normal precipitation in the extra-Carpathian and below (above) normal precipitation in the intra-Carpathian region. The SLP pattern explains 35% of the total SLP variance, whereas the precipitation pattern explains 17% of the total precipitation variance. It is also noted that the patterns of the two CCA pairs are

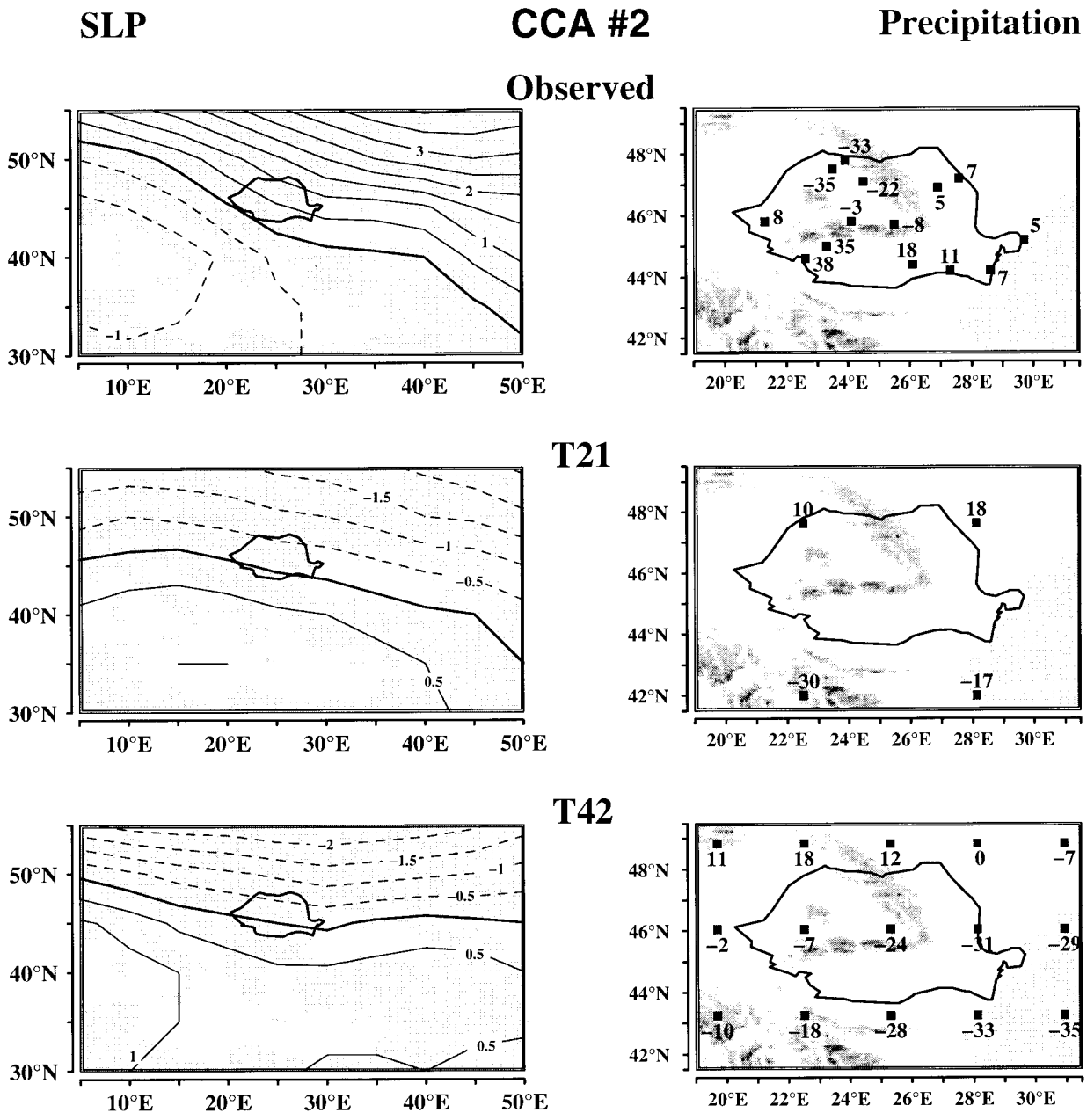

FIG. 8. As in Fig. 7 but for the second CCA pair.

similar to the first and second EOFs for both variables (Figs. 3–6), respectively (up to a change of sign, which is not relevant for linear techniques like EOF and CCA).

For the other seasons (not shown) the main mechanisms of this link are also plausible from a physical point of view but they are not related to the principal modes of the SLP variability (given by the first EOF), although, for precipitation, these patterns are similar. During spring, above (below) normal precipitation is maximally correlated to a cyclonic northwesterly (anticyclonic southeasterly) circulation over Europe (correlation coefficient of 0.76). In the summertime (Busuioc and von Storch 1995) above- (below-) normal precipitation over Romania goes along with a cyclonic (anticyclonic) structure centered over the Black Sea (correlation coefficient of 0.75). During autumn, the first CCA pair associates below- (above-) normal precipitation in Romania to an anticyclonic (cyclonic) structure over the northern part of Romania (correlation coefficient of 0.84).

All these CCA patterns are similar to the ones computed from the 1901–40 interval, except for spring. For winter and summer, they are also similar to the patterns discussed in Busuioc and von Storch (1995, 1996) for

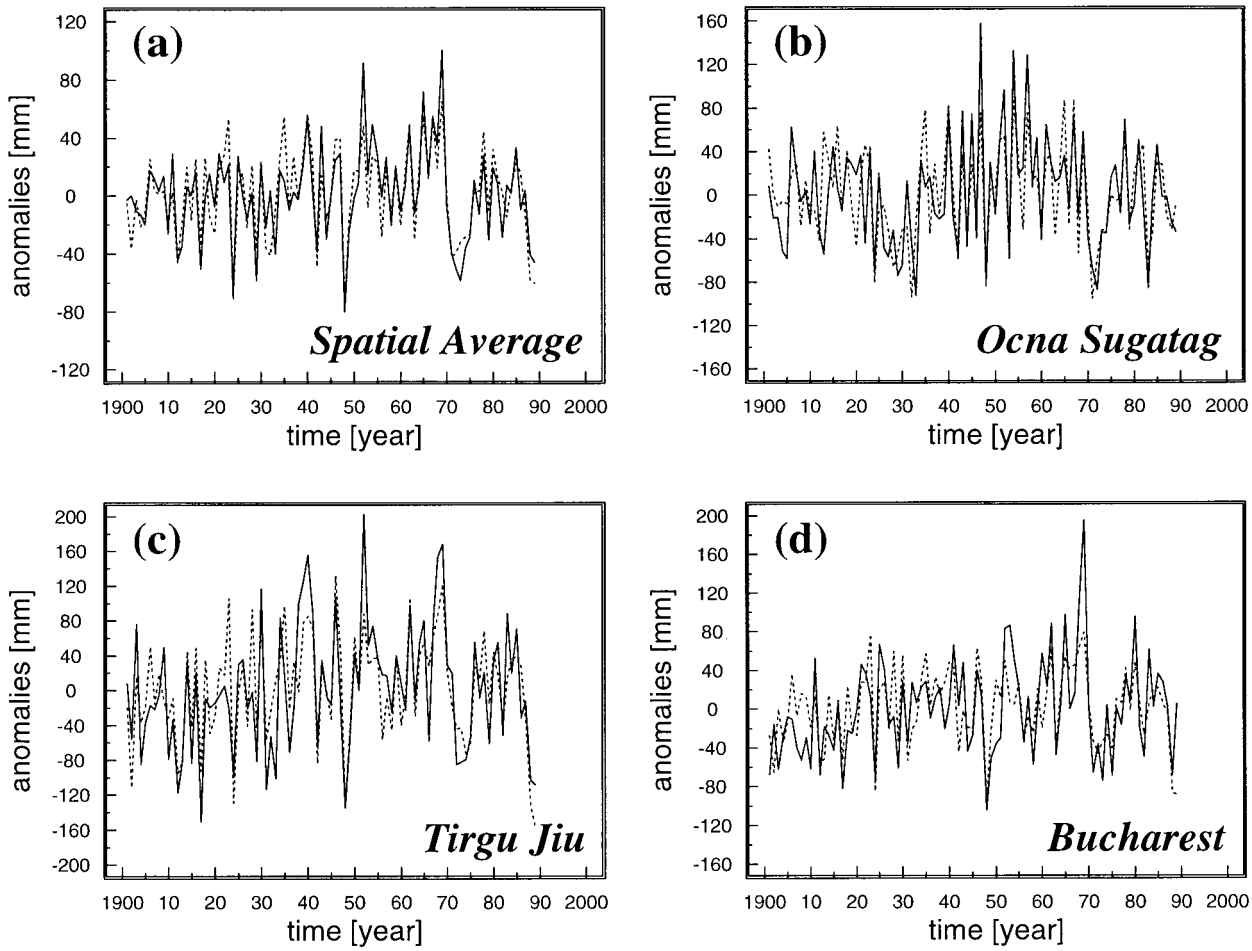

FIG. 9. Winter precipitation anomalies for 1901–1990 as derived from local station measurements (solid line) and as derived indirectly from the observed European-scale SLP anomalies by using the downscaling model (dashed line). Given are the spatial average for all 14 stations (a) as well as the anomalies for 3 individual stations: Ocna Sugatag (b), Tg. Jiu (c), and Bucharest (d).

the whole 1901–90 period. We conclude that the connection between local precipitation and the large-scale circulation did not substantially change during the last century, except for spring. This is very important for the derivation of a reliable statistical downscaling model. In fact, the instability of the spring patterns caused the validation of the downscaling models for the independent periods to fail (cf. Table 1), so that, for spring, no skillful model could be found.

Figure 9 illustrates as an example the application of the downscaling model induced by the empirical link described above to the observed 1901–90 SLP anomalies in winter at the European scale. Note that, for this application, the trend was not removed from the SLP time series. Figure 9a shows the spatial average of the local precipitation at the 14 Romanian stations as observed and as reconstructed by the downscaling model, Figs. 9b–d show the same information for three individual stations situated in different topographical environments: Ocna Sugatag, Tg. Jiu, and Bucharest. There is no substantial trend in both observed and estimated time series, and the interannual variations are generally reproduced by the downscaling model indicating its skill in winter. There are some more discrepancies for the individual stations, which is to be expected due to local (e.g., orographic) effects.

b. GCM simulated link: Verification of regional GCM simulations

The CCA analysis presented in section 5a for the observed data was repeated for the T21 and T42 GCMs using the models' gridpoint precipitation and SLP fields. Again displaying only results for the winter example, the middle and bottom rows of Figs. 7 and 8 present the first and second CCA pairs derived from the T21 and T42 GCM grid points, respectively. For both GCMs, the patterns for both SLP and precipitation coincide fairly well with those derived from the observations (neglecting the reversed signs of the T21 pattern in Fig. 7 and of the T21 and T42 patterns in Fig. 8 with respect to the observed patterns). Again, the role of the Car-

pathians in separating positive and negative anomalies is underrepresented in the second CCA precipitation patterns of the models. In both models, the correlation coefficient between SLP and precipitation patterns is about 0.91 for the first and about 0.81 for the second CCA pair. The explained variance of the first CCA SLP pattern is overestimated by the T42 model (59% against 36% observed), possibly due to the overestimation of the explained variance of the first SLP EOF used in the CCA. The variance explained by the first CCA SLP pattern derived from the T21 simulations is underestimated against observations. Both models underestimate the variance explained by the second CCA pair.

For the other seasons, the link between SLP and regional precipitation is strong as well although it does not reproduce the observed one in all cases even if it shows a physically reasonable mechanisms. In summary, the empirical link is correctly reproduced by the T42 model for winter and autumn and partially for spring (only first CCA pair). The T21 model captures the observed link for winter and spring and partially for summer (only first CCA pair). Thus, the two models may be considered skillful with respect to regional precipitation anomalies during these seasons. This statement does not affect the ability of the GCMs to correctly simulate the mean regional precipitation climate; that is, the models might still have a bias with respect to regional precipitation. As was discussed in section 4a this is, in fact, the case for some seasons in either the T21 or T42 model. Notwithstanding such model deficiencies, it has been demonstrated that downscaling methods can be useful tools for assessing the performance of GCMs on the regional scale. A similar technique has been used by Noguer (1994).

6. Changes in Romanian precipitation due to doubled CO_2 concentrations

A major caveat in any estimation of climate change, whether derived from statistical or dynamical models, is the fact that the parameters of these models are fitted to current climate conditions. In climate models, this is done by representing subgrid-scale processes through empirical parameterizations that are calibrated against the present-day climate. In statistical downscaling models, regional variables are parameterized directly by large-scale climate variables. These parameterizations represent empirical relationships that are not known to remain valid in changed climates. This is particularly a problem in downscaling applications where only a single relationship is considered (in our case the SLP–precipitation relationship), possibly missing other processes that determine the local variable in a changed climate (e.g., water vapor processes). On the other hand, global climate models consider many more processes and the complex interactions between them. Once we have verified that a GCM adequately represents a regional climate parameter such as precipitation, and thus many processes determining this parameter, we might place more confidence into climate change estimates for this local parameter simulated by the GCM. Therefore, we propose that such regional climate change estimates derived from GCMs proven as being reliable can be used to support the assumption that a downscaling model remains valid under a changed climate.

In this section, we illustrate this approach by considering estimated changes in the seasonal precipitation in Romania due to doubled CO_2 concentrations. The changes derived directly from the gridpoint precipitation simulated by the T21 and T42 models are presented and then compared to the changes derived indirectly by using the downscaling model. This comparison is useful only for the skillful downscaling models (i.e., all seasons except spring) and for reliable GCMs with respect to regional precipitation. The T21 and T42 climate models are considered reliable if they reproduce the observed large-scale flow variability (given by the most important EOFs of SLP; section 4) as well as the link between SLP and regional precipitation variability (given by the most important CCA pairs; section 5). These conditions are satisfied by the T42 model for winter and autumn. The T21 model reproduces the first two EOFs in winter and summer but only the first CCA in summer. Therefore, only the winter season is considered here.

Figure 10 (right column) shows the changes of winter precipitation in Romania as derived from the gridpoint precipitation of the T21 and T42 models ($2 \times CO_2$ minus control). The statistical significance of these differences has been tested using the adjusted *t*-statistic, which explicitly takes into account serial correlation (Zwiers and von Storch 1995). As noted earlier the gridpoint precipitation should be interpreted as representing areal averages, also the results for the T21 model should be considered with caution since it is difficult to derive Romanian estimates from the four grid points present in that model. From both models we can infer approximately the same overall climate change signal: a moderate increase in the northwestern part of Romania and a decrease in the south and southeast. The differences in the T21 model are not statistically significant, whereas, for the T42 model, they are significant at the 5% level only in the southeastern part.

The downscaling model derived from the observed link between large-scale circulation and regional precipitation has been applied to the $2 \times CO_2$ SLP anomalies computed relative to the control runs. The climate change signal is presented in terms of the long-term mean of the downscaled precipitation anomalies. The results are shown in the left column of Fig. 10. An agreement between the gridpoint signal and the downscaled signal can be noted—namely, an increase in the northwestern region and a decrease in the rest of the country (except for the T21 model, which shows an increase at the Black Sea coast). The agreement is less convincing for the T21 model, which might be due to the fact that this model only partially reproduces the

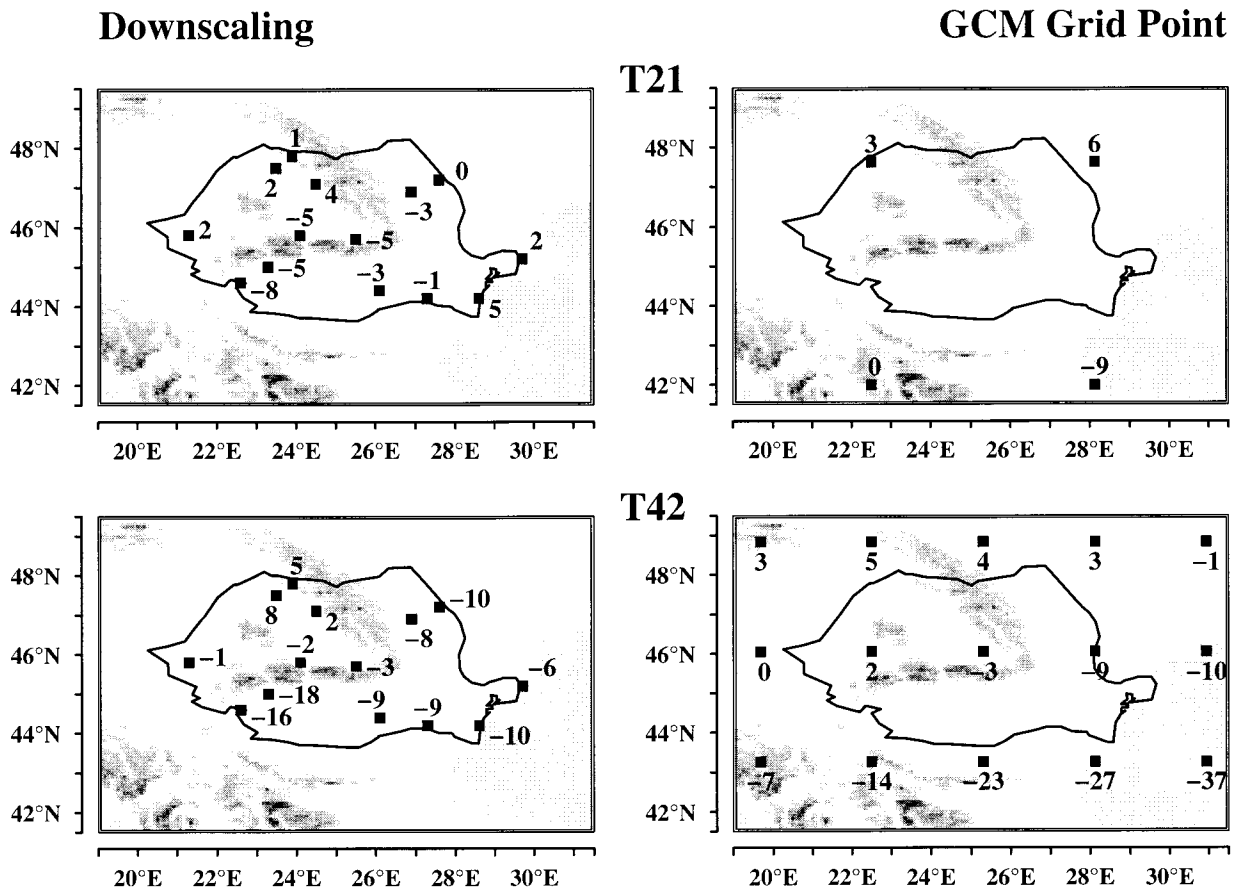

FIG. 10. Changes due to doubling CO_2 of winter precipitation in Romania as derived from the ECHAM3 T21 (top row) and T42 (bottom row) time-slice experiments. The changes derived directly from the gridpoint precipitation of the GCMs (right column) are differences between the means from the $2 \times CO_2$ and the $1 \times CO_2$ experiments. The climate change signal displayed in the left column represents the long-term mean of the downscaled precipitation anomalies derived indirectly from the GCM-simulated European-scale SLP anomalies ($2 \times CO_2$ minus $1 \times CO_2$).

large-scale SLP variability: it overemphasizes an almost zonal flow pattern over Europe and underestimates the importance of the most important EOF with a cyclonic northwesterly flow over Romania (see section 4c).

In summary, we showed that the downscaled climate change signal for regional precipitation is similar to the signal directly obtained from the GCM grid points (especially the T42 model). We argue that this might be considered to support the notion that the empirical link between large-scale SLP and precipitation continues to characterize an important mechanism under changed climate conditions, at least the $2 \times CO_2$ climate of the ECHAM3 models. Thus, the downscaling model seems to be applicable to derive climate change scenarios at local stations in Romania from GCM climate change experiments.

One difficulty in the above approach results from the differences in the data type represented in the left and right columns of Fig. 10—that is, the fact that the GCM-derived patterns of precipitation change are represented on a gridpoint basis while the changes derived indirectly from the downscaling model are given in terms of station precipitation. An alternate way of testing whether the circulation–precipitation link remains unchanged in a perturbed climate would be to develop the CCA link from the control integration of the GCM and apply the resulting downscaling model to SLP from the perturbed GCM runs to predict perturbed grid-box precipitation. These changes could be directly compared to the gridpoint precipitation simulated by the GCM. This approach, however, would involve a more detailed comparative study of the performance of the control integration with respect to the observed climate and is therefore reserved for a follow-up study.

7. Conclusions

The purpose of the present paper is twofold: first, a downscaling technique is used as a diagnostic tool to verify the performance of climate models on the regional scale under present-day climate conditions; second, a technique for verifying the applicability of em-

pirical downscaling procedures in climate change applications is proposed. The case considered is seasonal precipitation in Romania; the downscaling model consists of a linear regression based on canonical correlation analysis (CCA) using European-scale air pressure fields as predictors. The climate models are the T21 and T42 versions of the ECHAM3 atmospheric GCM. The climate change scenario refers to the expected time of doubled carbon dioxide around 2050.

The general features of the spatial variability of seasonal precipitation in Romania are reproduced fairly well by the T21 and T42 ECHAM3 simulations for all seasons in spite of the highly irregular topography of the region—namely, the decrease of precipitation amount from west to east, the uniform sign for the first EOF and a northwest–southeast opposite sign structure for the second EOF. However, some details are not reproduced because of the coarse spatial resolution of the models. Also, the seasonal cycle is not correctly reproduced by the models. Only the T21 model captures the maximum precipitation in summer and the minimum in autumn.

The link between seasonal precipitation variability in Romania and European SLP variability given by the CCA is strong for all seasons, especially for winter and autumn. This link appears to be primarily related to the first SLP EOF only for the winter season. For the other seasons, the main mechanism of this link is related to the regional SLP patterns. By considering two independent subintervals, 1901–40 and 1941–90, of the observational period it was found that, in the past century, this connection was maintained unchanged in time for all seasons except for spring. Consequently, defining skill in terms of the subinterval independent from the fitting interval, the downscaling model, which is built on the basis of this link is skillful for all seasons but spring.

The GCMs reproduce these links for winter and autumn (T42), respectively, winter and spring (T21) (the 1941–90 link in case of spring). Thus, during these seasons, these climate models may be considered skillful in simulating the mechanisms that control regional precipitation through the large-scale circulation.

The large-scale SLP variability given by the first two EOF patterns is reproduced by both models in winter. Therefore, for this season the change of precipitation due to doubled CO_2 concentrations was estimated (using the downscaling model derived from observations) and compared with the GCM estimates derived directly from the gridpoint data. The two signals are consistent (especially for T42 model) and show an increase of precipitation in the northwestern region and a decrease in the rest of the country. Thus, it can be concluded that the downscaling technique is adequate for describing climatically changing regional and local conditions in Romania in winter. The rationale for this conclusion is given by the following line of arguments: 1) for present-day climate conditions, the downscaling model (or, equivalently, the CCA patterns) was proven to be skillful for this season in representing local and regional precipitation through its link to the large-scale circulation; 2) by comparing this observed with the GCM-simulated link it was shown that the GCMs are reliable in modeling regional precipitation and the processes determining the link between precipitation and the large-scale circulation; 3) because the GCMs consider many more processes than the statistical downscaling model we are more confident that the GCMs are also reliable in climate change applications; 4) if the downscaled climate change estimates can be shown to be similar to the GCM-simulated changes on a regional scale, we argue that the (single) relationship used in the downscaling approach will continue to account for a large part of the precipitation variability under changed climate conditions and that the observed link can be used to estimate local and regional precipitation from large-scale SLP taken from GCM climate change experiments.

It is stressed that this approach is not *proof* that the downscaling technique can be used for changed climates, we argue only that, if the similarity in argument 4 can be demonstrated, it is more likely that the empirical relationship remains valid. We therefore believe that this is an improvement in the sense of *increased confidence* over the mere assumption commonly made in downscaling studies that the downscaling relationship can still be used in changed climates. Even if the GCM-simulated and downscaled regional changes are similar it might be the case that both models are wrong for the changed climate because both the empirical parameterizations in the GCM and the single empirical relationship in the downscaling model might not be valid anymore. But under this scenario it would be unlikely that the complex interactions in the GCM between a multitude of processes influencing precipitation—respectively, the single relationship in the downscaling model—would yield the same, but wrong, result. If, for a climate change experiment, the GCM-simulated and downscaled estimates are different, no conclusions can be drawn about the validity of either model. It could be that the GCM is correct but the single relationship (e.g., SLP–precipitation), and thus the downscaling model, is not sufficient to represent regional precipitation. On the other hand, it is also possible that the downscaling relationship remains valid but some other parameterizations in the GCM do not.

It might be interjected that, if a reliable GCM is available, why bother with the downscaling. There are two reasons why downscaling is still useful and even needed. First, in the introduction we distinguished between the skill, or lack thereof, of climate models on the large, the regional, and the local scale. GCMs are considered to have skill on the large and no skill on the local scale. They might be skillful on the intermediate, regional scale but this is not a priori clear. In the case considered above, the GCMs were indeed shown to be reliable on the regional scale with respect to precipitation in Ro-

mania. However, (statistical) downscaling methods are still required to obtain estimates at the local (station or subgrid) level, both for present and future climate conditions. Second, in section 6 it was demonstrated how relatively cheap ($1 \times CO_2$ and $2 \times CO_2$ time slice) GCM experiments can be used to support the assumption that the statistical downscaling relationship remains valid under changed climate conditions. This result suggests that the downscaling procedure might be applied to (long) transient GCM experiments with gradually increasing CO_2 concentrations. Thus, the downscaling technique appears as cost-effective alternative to computationally expensive downscaling approaches with regional or global high-resolution dynamical models.

Acknowledgments. This study was made possible through funding from the German Ministry of Education, Science, Research and Technology BMBF (Project 07VKV01/1) and the Max-Planck-Gesellschaft, which financed two extended visits of Dr. A. Busuioc to the Max-Planck-Institut für Meteorologie in Hamburg. The final version of this paper was prepared during a visit to the Institute of Hydrophysics, GKSS Research Center in Geesthacht, Germany. The third author was supported through Project 01LK9510/0 of the BMBF and the five coastal states of northern Germany.

The authors thank Dr. U. Cubasch for the permission to use data from the GCM time-slice experiments performed at the German Climate Computing Center. Dr. V. Kharin and M. Junge helped to extract the GCM data. Dr. E. Zorita and H. Heyen helped with computational routines and by providing the SLP analyses fields for Europe.

APPENDIX

Selection of CCA Model

In this appendix, the selection procedure for the optimum number of EOF and CCA components in the construction of the statistical downscaling model is presented. As discussed in section 3, the skill of the model depends on the number of EOFs retained for the CCA analysis as well as the number of CCA time series used in the regression model. The sensitivity of the skill against the choice of the fitting interval is also discussed.

We use a split-sampling approach by dividing the complete interval 1901–90 into two subintervals 1901–40 and 1941–90. First, the downscaling model is fitted by estimating the EOFs and CCAs from the 1941–40 interval and validated for the independent dataset from the 1901–40 period (*variant 1*). Then the situation is reversed, the model being fitted from the 1901–40 data and validated for 1941–90 (*variant 2*). The skill of the model is expressed by two measures: the fraction of total observed variance explained by the reconstructed (downscaled) precipitation values, and the correlation coefficient between the reconstructed and observed precipitation time series (averages over all stations, respectively). Table 1 lists these measures of skill separately for the fitting and validation intervals, by using different combinations of EOF and CCA patterns. Only EOFs that explain at least 1% from the total variance are considered. For the same number of EOFs, the skill is highest for the maximum number of CCA patterns (i.e., to the number of EOFs) used in the regression model, or one less in three cases. For the sake of brevity, only these cases are presented in Table 1. Other studies revealed that, in some cases, a smaller than the maximum number of CCA time components might be sufficient for a good skill (cf. von Storch et al. 1993; Werner and von Storch 1993; Heyen et al. 1996).

In general, the skill of the model for the fitting period increases with the number of EOFs retained for the CCA analysis. The optimum combination of EOFs and CCAs used was determined in such a way that either the skill for the two validation periods (respectively, their average) reaches a maximum, or that an increase by one EOF (CCA) would change the skill only by a small amount.

For example, looking at the validation interval 1941–90 in the case of winter (last column), retaining five EOFs for SLP and precipitation for the CCA analysis and using five CCA time series in the regression model seems to be the optimum combination since the skill (explained variance of 0.62 and correlation coefficient of 0.82) changes only a little by using more components. However, for the 1901–40 validation interval, the explained variance for this combination is much smaller than for the case of six EOFs and six CCAs (0.28 against 0.41). On average, using both validation intervals and both measures of skill, this latter combination is optimal. Surprisingly, for variant 2 the skill for the validation interval is higher than for the fitting interval. This might be explained by the high quality of data during the 1941–90 period and the small number of missing data. The optimum combinations used in this paper are highlighted in boldface in Table 1. For spring, no model with an acceptable skill for the validation period exists, although the correlation coefficients for the first two CCA pairs are close to, for instance, the summer values (also manifested in the reasonable skills for the fitting intervals in spring, see Table 1). Obviously, this is due to the fact that, for spring, the first two CCA pairs are different for the two subintervals (as presented in section 5) so that the link between regional precipitation and large-scale circulation is not stable over time. As a result, the skill of the model breaks down if derived from the independent validation subintervals.

It can also be seen from Table 1 that the skill of the downscaling model for winter is reasonably high even if only the first two EOFs are retained for the CCA, whereas, for summer and autumn, more EOFs are necessary to obtain high skills. This might be due to the fact that, for winter, the link between local precipitation and large-scale circulation (in terms of the first two CCA

pairs) is primarily related to the first SLP EOF and secondarily to the second SLP EOF. These two patterns account for 71% of the total SLP variance. For the other seasons, the main mechanisms of this link are not related to the principal modes of SLP variability (given by first EOF) even though, for precipitation, the EOF and CCA patterns are similar. Also, the correlation coefficients for the second CCA pairs are not as high as during wintertime.

REFERENCES

Barnett, T., and R. Preisendorfer, 1987: Origin and levels of monthly and seasonal forecast skill for United States surface air temperatures determined by canonical correlation analysis. *Mon. Wea. Rev.*, **115,** 1825–1850.

Bengtsson, L., M. Botzet, and M. Esch, 1995: Hurricane-type vortices in a general circulation model. *Tellus*, **47A,** 175–196.

Bürger, G., 1996: Expanded downscaling for generating local weather scenarios. *Climate Res.*, **7,** 11–28.

Busuioc, A., 1994: The influence of the Carpathian mountains to the variability of the Romanian precipitation in wintertime. *Ann. Meteor.*, **30,** 247–250.

——, and H. von Storch, 1995: The connection between summer precipitation anomalies in Romania and large-scale atmospheric circulation. *Proc. Atmospheric Physics and Dynamics in the Analysis and Prognosis of Precipitation Fields*, Rome, Italy, 369–373.

——, and ——, 1996: Changes in the winter precipitation in Romania and its relation to the large scale circulation. *Tellus*, **48A,** 538–552.

Conway, D., R. L. Wilby, and P. D. Jones, 1996: Precipitation and air flow indices over the British Isles. *Climate Res.*, **7,** 169–183.

Cubasch, U., K. Hasselmann, H. Hoeck, E. Maier-Reimer, U. Mikolajewicz, B. D. Santer, and R. Sausen, 1992: Time-dependent greenhouse warming computations with a coupled ocean–atmosphere model. *Climate Dyn.*, **8,** 55–69.

——, H. von Storch, J. Waskewitz, and E. Zorita, 1996: Estimates of climate change in Southern Europe using different downscaling techniques. *Climate Res.*, **7,** 129–149.

Cui, M., H. von Storch, and E. Zorita, 1995: Coastal sea level and the large-scale climate state. A downscaling exercise for the Japanese Islands. *Tellus*, **47A,** 132–144.

Draghici, I., 1988: *Dynamics of Atmosphere* (in Romanian). Ed. Acad. R.S.R., 475 pp.

Fuentes, U., and D. Heimann, 1996: Verification of statistical-dynamical downscaling in the Alpine region. *Climate Res.*, **7,** 151–168.

Gyalistras, D., H. von Storch, A. Fischlin, and M. Beniston, 1994: Linking GCM-simulated climatic changes to ecosystem models: Case studies of statistical downscaling in the Alps. *Climate Res.*, **4,** 167–189.

Harrison, P. A., R. E. Butterfield, and T. E. Downing, 1995: Climate change and agriculture in Europe. Assessment of impacts and adaptation. Research Rep. 9, Environmental Change Unit, University of Oxford, 411 pp.

Hewitson, B. C., and R. G. Crane, 1996: Climate downscaling: Techniques and applications. *Climate Res.*, **7,** 85–95.

Heyen, H., E. Zorita, and H. von Storch, 1996: Statistical downscaling of monthly mean North Atlantic air-pressure to sea level anomalies in the Baltic Sea. *Tellus*, **48A,** 312–323.

Kaas, E., T.-S. Li, and T. Schmith, 1996: Statistical hindcast of wind climatology in the North Atlantic and northwestern European region. *Climate Res.*, **7,** 97–110.

Karl, T. R., W. C. Wang, M. E. Schlesinger, R. W. Knight, and D. Portman, 1990: A method of relating general circulation model simulated climate to the observed local climate. Part I: Seasonal statistics. *J. Climate*, **3,** 1053–1079.

Katz, R. W., and M. B. Parlange, 1996: Mixtures of stochastic processes: Applications to statistical downscaling. *Climate Res.*, **7,** 185–193.

Noguer, M., 1994: Using statistical techniques to deduce local climate distributions. An application for model validation. *Meteor. Apps.* **1,** 277–287.

Osborn, T. J., and M. Hulme, 1997: Development of a relationship between station and grid-box rainday frequencies for climate model evaluation. *J. Climate*, **10,** 1885–1908.

Roeckner, E., 1992: Simulation of the present-day climate with the ECHAM model: Impact of model physics and resolution. Report 93, Max-Planck-Institut für Meteorologie, 171 pp. [Available from Max-Planck-Institut für Meteorologie, Bundesstr. 55, D-20146 Hamburg, Germany.]

Trenberth, K. E., and D. A. Paolino, 1980: The Northern Hemisphere sea-level pressure data set: Trends, errors and discontinuites. *Mon. Wea. Rev.*, **108,** 855–872.

von Storch, H., 1995a: Spatial patterns: EOFs and CCA. *Analysis of Climate Variability: Application of Statistical Techniques*, H. von Storch and A. Navara, Eds., Springer-Verlag, 227–258.

——, 1995b: Inconsistencies at the interface of climate impact studies and global climate research. *Meteor. Z.*, **4,** 72–80.

——, E. Zorita, and U. Cubasch, 1993: Downscaling of global climate change estimates to regional scale: An application to Iberian rainfall in wintertime. *J. Climate*, **6,** 1161–1171.

Werner, P., and H. von Storch, 1993: Interannual variability of central european mean temperature in January–February and its relation to large-scale circulation. *Climate Res.*, **3,** 195–207.

Wigley, T. M. L., P. D. Jones, K. R. Briffa, and G. Smith, 1990: Obtaining subgrid scale information from coarse-resolution general circulation model output. *J. Geophys. Res.*, **95,** 1943–1953.

Zwiers, F. W., and H. von Storch, 1995: Taking serial correlation into account in test of the mean. *J. Climate*, **8,** 336–351.